J Mater Sci (2010) 45:3661–3670
DOI 10.1007/s10853-010-4411-x

Formation of calcium phosphates on low-modulus Ti–7.5Mo alloy by acid and alkali treatments

Hsueh-Chuan Hsu · Shih-Ching Wu · Chao-Lun Fu · Wen-Fu Ho

Received: 13 December 2009 / Accepted: 11 March 2010 / Published online: 30 March 2010

Abstract This study investigated the hydroxyapatite (HA) coating on metal implants in order to enhance their bioactive properties. In this study, HA coatings were formed on the surfaces of commercially pure titanium (c.p. Ti) and Ti–7.5Mo which were acid-etched and subsequently alkali-treated before samples were soaked in simulated body fluid (SBF). Specimens of c.p. Ti and Ti–7.5Mo were etched in either H_3PO_4 or HCl, and subsequently treated in NaOH. The surfaces of acid-etched c.p. Ti showed a porous structure, whereas those of acid-etched Ti–7.5Mo showed some grinding marks, but no porosity. After subsequent alkali treatment in NaOH, the surfaces of both the c.p. Ti and Ti–7.5Mo substrates exhibited microporous network structures. The specimens were then immersed in SBF at 37 °C for 28 days. Apatite began to deposit on acid-etched and NaOH-treated Ti–7.5Mo within 1 day after immersion in the SBF. After 28 days of immersion in the SBF, a dense and uniform layer was produced on the surfaces of all samples. The HA formation rate was the highest for HCl and NaOH-pretreated samples, and the results of EDS and XRD showed that much more intensive peaks of HA appear on the specimens of HCl and NaOH-treated Ti–7.5Mo than on any other sample. Thus, this method of apatite coating Ti–7.5Mo appears to be promising for artificial bone substitutes or other hard tissue replacement materials with heavy load-bearing applications due to their desirable combination of bioactivity, low elastic modulus, and low processing costs.

H.-C. Hsu · S.-C. Wu
Department of Dental Laboratory Technology, Central Taiwan University of Science and Technology, Taichung, Taiwan, ROC

H.-C. Hsu · S.-C. Wu
Institute of Biomedical Engineering and Material Science, Central Taiwan University of Science and Technology, Taichung, Taiwan, ROC

C.-L. Fu · W.-F. Ho (✉)
Department of Materials Science and Engineering, Da-Yeh University, No. 168, University Road, Dacun, Changhua 51591, Taiwan, ROC
e-mail: fujii@mail.dyu.edu.tw

Introduction

Titanium and titanium alloys are widely used for biomedical and dental implants for their superior mechanical properties. But while they are biocompatible, they cannot bond directly to bone. After implantation into a living body, bio-inert titanium-based materials are generally encapsulated by fibrous tissue that isolates them from the surrounding bone [1, 2]. This type of capsule inhibits proper biomechanical fixation and leads to clinical failure of the implant. In contrast, it is well recognized that calcium phosphate coatings have better long-term clinical success rates than uncoated titanium implants [3, 4], and various surface modifications have been applied to the metal to enhance bone induction and conduction around the implants. For example, plasma-spraying, sputter-deposition, sol–gel coating, electro-deposition, or biomimetic precipitation [5–12]. Of all the choices now available, plasma-sprayed hydroxyapatite (HA) is the most successful and widely applied coating [11]. However, plasma-spraying is a line-of-sight technique and cannot uniformly coat internal surfaces, such as the porous bead coatings on joint implants [13]. In addition, the high-temperature plasma flame may cause HA input powders to decompose into other phases such as tricalcium phosphate and calcium oxide [14, 15].

Due to their biocompatibility, bioactivity, and osteoconduction, calcium phosphate materials have strong

applications in the field of biomaterials, such as bone substitution and repair. Most recently, new synthetic methods of calcium phosphates as biomaterials have been developed, such as lamellar mesostructured calcium phosphate [16] and hydrothermal synthesis of HA whiskers [17]. Also, there has been great interest in the use of calcium phosphates as scaffolding materials for bone tissue engineering. The development of tissue engineering scaffolds based on polymer-coated bioceramics and interpenetrating polymer/bioceramic microstructures has also been presented by Yunos et al. [18]. Additionally, Costa et al. [19] have developed a three-dimensional macroporous alumina scaffold with a biocompatible PVA/calcium phosphate coating. Furthermore, a recent report by MacKenzie et al. [20] indicate that potassium aluminosilicate inorganic polymers containing 10 wt% $Ca(OH)_2$, nanostructured calcium silicate, and $Ca_3(PO_4)_2$ appears to be promising as a bioactive biomaterial.

Alternatively, it has been reported that a bioactive titanium surface can be prepared by means of a simple chemical treatment in NaOH [21, 22], and the chemical modification of titanium surfaces has attracted much attention due to its simplicity, effectiveness, and applicability to implants with irregular shapes [23–29]. To date, the structural changes in a titanium surface during chemical treatment and the subsequent apatite formation in simulated body fluid (SBF) have been described in a number of studies [21–29]. In fact, some studies have achieved a higher bone-to-implant contact for biomimetic calcium phosphate coatings than for uncoated titanium implants [5, 30].

In the past few years, new Ti alloys have been intensively investigated and developed for biomedical applications as possible substitutes of the well-established Ti–6Al–4V alloy [31–33]. Though Ti–6Al–4V presents excellent mechanical and corrosion properties, it contains vanadium, which is known to be cytotoxic [34]. Thus, avoiding metal ion release and obtaining vanadium-free alloys with similar properties has been the focus of recent investigations [35–37]. Another important requirement for implants designed to replace or interact with bone is a low elastic modulus matching, as closely as possible, that of the surrounding bone tissue [38–40].

Ti–7.5Mo has been reported to show much better corrosion resistance [41], mechanical properties [42], and cytocompatibility [43] than Ti–6Al–4V. Moreover, α''-phase Ti–7.5Mo alloy exhibits a lower elastic modulus which can reduce the stress-shielding effect [39, 40]. However, like other biomedical titanium alloys, it remains a bio-inert material. Thus, the apatite-forming ability of Ti–7.5Mo treated with either HCl or H_3PO_4, before immersion in NaOH aqueous solution and then SBF was investigated in this study. The results were compared with those of commercially pure titanium (c.p. Ti) chosen as a control. Because the acid and alkali treatments do not involve high-temperature processes, this method is especially suitable for the metastable α''-phase Ti–7.5Mo alloy which is sensitive to temperature. In fact, a high-temperature treatment process after chemical treatment results in the crystallization of the hydrogel layer, hence reducing the ionic activity and decreasing the rate of apatite nucleation and formation [44]. In addition, since it is known that an essential requirement for an artificial material to bond to living bone is the formation of a bonelike apatite layer on its surface in the body environment [45, 46], this process could make the Ti–7.5Mo alloy an attractive biomaterial.

Experimental procedures

The materials used for this study were c.p. Ti and a Ti–7.5Mo alloy. (*Note*: all compositions are expressed in mass.) All the materials were prepared from raw titanium (99.8% pure) and molybdenum (99.95% pure) by using a commercial arc-melting vacuum–pressure-type casting system (Castmatic, Iwatani Corp., Japan). The ingots of approximately 30 g each were re-melted thrice, for about 55 s each, to improve their chemical homogeneity. Prior to casting, the ingots were again re-melted. The difference in pressure between the two chambers allowed the molten alloys to instantly drop into a graphite mold at room temperature. In this study, the cast alloys were sectioned using a Buehler Isomet low-speed diamond saw to obtain specimens. Flat sheets of c.p. Ti and of Ti–7.5Mo, $1 \times 10 \times 10$ mm^3 in size, were used as substrate materials. The surfaces of the metals were abraded to the final level of a 2000-grit paper. The metal substrates were then ultrasonically cleaned in distilled water, acetone, and ethanol for 20 min each, after which the substrate plates were again cleaned in distilled water for another 10 min.

Two different acid etching procedures were performed: (i) samples were etched in 35% HCl for 2 h at room temperature (about 20 °C), and (ii) samples were etched in 85% H_3PO_4 for 2 h at room temperature. After etching, all specimens were immersed in 15 M NaOH aqueous solution at 60 °C for 24 h. The temperature was maintained by using a water bath. After the 24 h incubation period, the substrates were gently washed with distilled water and dried at 40 °C for 24 h. The surfaces of the specimens were then examined by scanning electron microscopy (SEM; JSM-6700F, JEOL, Japan) and X-ray diffractometry (XRD; D8 SSS, Bruker, Germany).

Contact angle measurements were implemented to evaluate the wettability of the c.p. Ti and Ti–7.5Mo specimens before and after the various treatments. An equal volume of distilled water was placed on each sample

Table 1 Ionic concentrations (mM) of SBF compared to human blood plasma [47]

	Na^+	K^+	Mg^{2+}	Ca^{2+}	Cl^-	HPO_4^{2-}	SO_4^{2-}	HCO_3^-
SBF	142.0	5.0	1.5	2.5	148.8	1.0	0.5	4.2
Blood plasma	142.0	5.0	1.5	2.5	103.8	1.0	0.5	27.0

by means of a micropipette, either forming a drop or spreading on the surface. A CCD camera was used to photograph the shape of the drops and measure the contact angle. Six specimens were used to evaluate the contact angles for each material type and experimental conditions.

To test the capability of the material to spontaneously form a bonelike apatite layer in vitro, the acid-etched and subsequently NaOH-treated c.p. Ti and Ti–7.5Mo substrates were soaked in a 20-mL SBF. The SBF was prepared by dissolving reagent grade NaCl, $NaHCO_3$, KCl, $K_2HPO_4{\cdot}3H_2O$, $MgCl_2{\cdot}6H_2O$, $CaCl_2$, and Na_2SO_4 into distilled water. The final ionic concentrations of the SBF (versus human plasma) are listed in Table 1 [47]. The temperature was maintained by using a water bath. The SBF was refreshed every 2 days to preserve its ion concentration. After being soaked for selected time periods (1, 7, 14, and 28 days), the specimens were removed from the fluid, washed with distilled water, and air-dried. Changes in the c.p. Ti and Ti–7.5Mo surfaces after chemical treatments and soaking in SBF were examined by SEM (S-3000N, Hitachi, Japan). After 28 days, the structural changes occurring on the surfaces due to the aforementioned procedures were investigated by means of XRD (D8 SSS, Bruker, Germany). The surface chemical analysis was implemented by energy-dispersive X-ray spectroscopy (EDS) coupled with the SEM.

Results and discussion

Characterization of surface

Figure 1 shows the SEM micrographs of c.p. Ti and Ti–7.5Mo substrates after surface treatment with acid etching and NaOH activation. Surfaces of c.p. Ti after acid etching in either H_3PO_4 or HCl showed a porous structure (Fig. 1a, c), however, those of Ti–7.5Mo showed some grinding marks and no porosity (Fig. 1b, d). After subsequent alkali treatment in NaOH, the surfaces of both the c.p. Ti and Ti–7.5Mo substrates exhibited microporous network structures, as shown in Fig. 1e–h. These results have been correlated with the high corrosion resistance of Ti–Mo alloys in various test solutions. For example, Zardiackas et al. [48] reported that the anodic polarization measurements of Ti–Mo alloy exhibited better resistance in a test corrosive environment than c.p. Ti, Ti–6Al–4V ELI and Ti–6Al–7Nb alloys. Moreover, the corrosion resistance of Ti–30Mo in 35% HCl was studied by electrochemical and open-circuit analysis by Sakaguchi et al. [49], and the results showed that this alloy is more resistant than c.p. Ti. The SEM observations indicated no structural differences on the surfaces of c.p. Ti and Ti–7.5Mo after acid etching and alkali treatment. A sodium titanate ($Na_2Ti_5O_{11}$) peak appeared between 29° and 30° in 2θ on all XRD patterns (figure not shown) after NaOH treatment of the c.p. Ti and Ti–7.5Mo surfaces, and the microporous network structures of metal surfaces after alkali treatment suggest the probable formation of a sodium titanate, which is in agreement with the results reported by Kim et al. [50].

Wettability

Surface wettability (generally referred to as hydrophobicity/hydrophilicity) is one of the most important parameters affecting the biological response to an implanted material. Wettability affects protein adsorption, platelet adhesion/activation, blood coagulation, and cell and bacterial adhesion [51–54]. Thus, highly hydrophilic surfaces seem more desirable than hydrophobic ones in view of their interactions with biological fluids, cells, and tissues [55, 56]. In a recent animal study, Buser et al. [55] found that a hydrophilic sandblasted/acid-etched surface promoted better enhanced bone apposition during the early stages of bone regeneration. We note that contact-angle measurements give values ranging from 0° (hydrophilic) to 140° (hydrophobic) for titanium implant surfaces [55, 57, 58].

Figure 2 shows the average water-contact angles of the c.p. Ti and Ti–7.5Mo specimens untreated, after acid etching in H_3PO_4 or HCl, and after subsequent alkali treatment in NaOH. Distilled water contacted the untreated samples of c.p. Ti and Ti–7.5Mo at about 23.2° and 22.6°, respectively, but after acid etching in H_3PO_4 or HCl, the water-contact angles of the surfaces slightly decreased. The results of Duncan's test showed that no significant difference was found in contact angles among the groups for either untreated or acid-etched surfaces ($p > 0.05$). After subsequent alkali treatment in NaOH, the surfaces of both the c.p. Ti and Ti–7.5Mo were much more easily wetted, thus resulting in a very low contact angle, and Duncan's test results indicated significant differences ($p < 0.05$) in the water-contact angles before and after alkali treatment for both the c.p. Ti and Ti–7.5Mo surfaces. It is worth noting that the acid-etched and NaOH-treated Ti–7.5Mo had significantly lower ($p < 0.05$) contact angles than pretreated c.p. Ti. Thus, the contact angles of alkali-treated Ti–7.5Mo were decreased to 6.4° and 3.5° after treatment with H_3PO_4 and HCl, respectively. Moreover, the water-

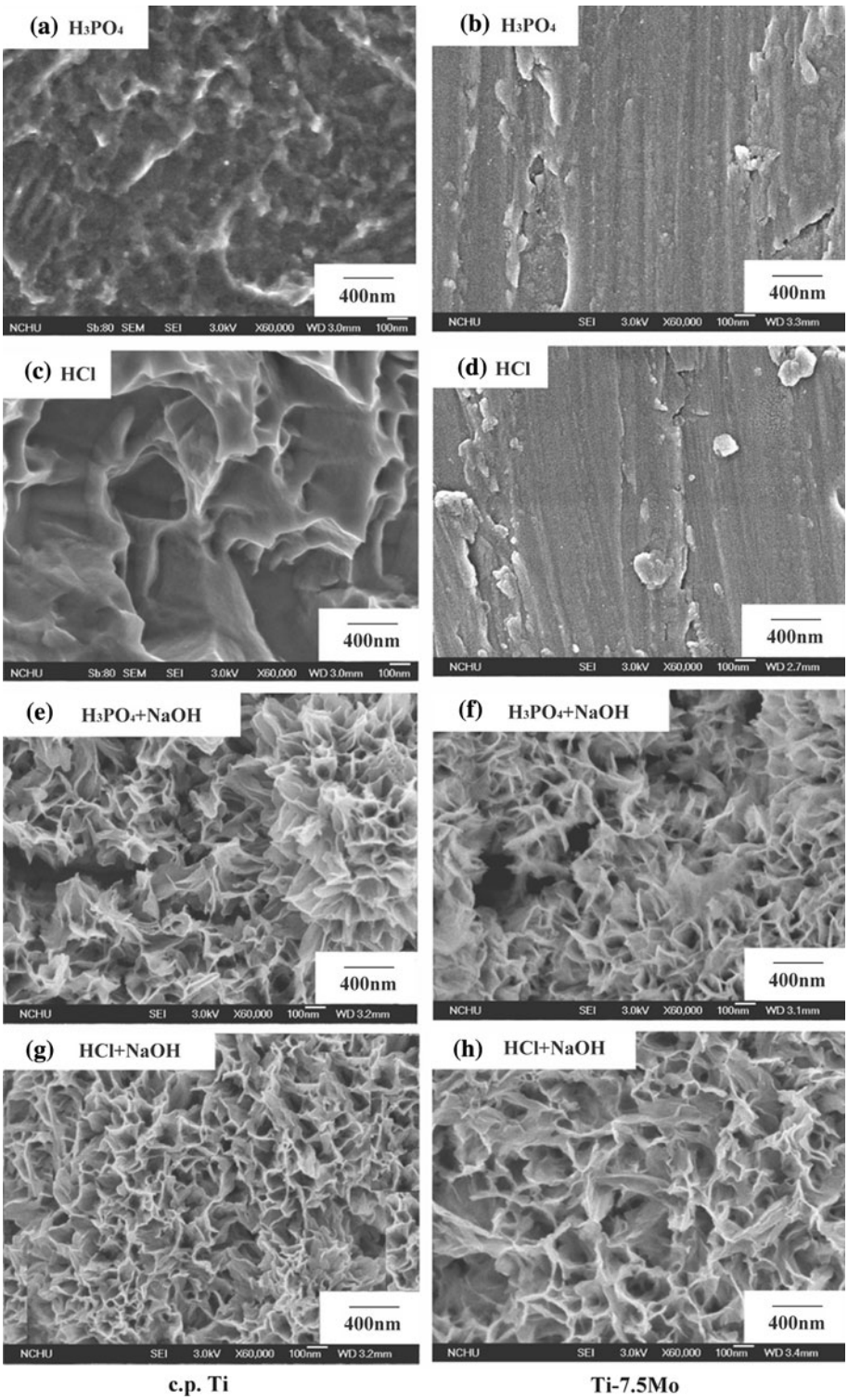

Fig. 1 SEM micrographs of surface morphology of chemically treated c.p. Ti (*left*) and Ti–7.5Mo (*right*)

contact angles of the surfaces of both metals were the smallest after HCl etching and subsequent NaOH treatment. Of all the test conditions, the Ti–7.5Mo surfaces after HCl etching in combination with the NaOH treatment had the lowest contact angles.

Ca–P precipitation on the chemically treated surfaces

To assess the bioactivity of the chemically treated c.p. Ti and Ti–7.5Mo surfaces, in vitro testing was performed in SBF. Figure 3 shows SEM photographs of the surfaces of the

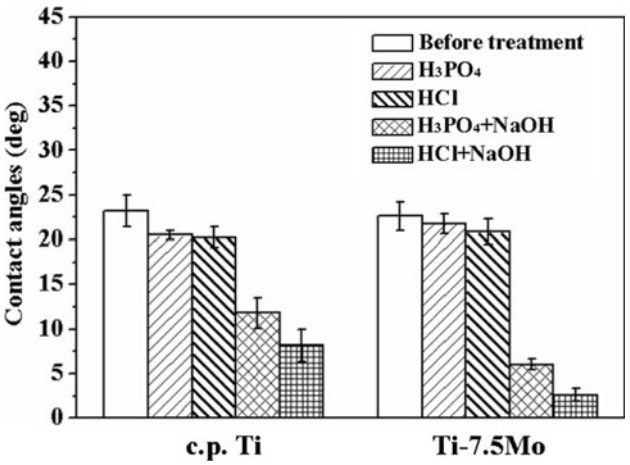

Fig. 2 Average water-contact angles of untreated and different chemically treated c.p. Ti and Ti–7.5Mo specimens

acid-treated c.p. Ti and Ti–7.5Mo samples that were immersed in the SBF. No precipitation appeared on the surfaces of c.p. Ti and Ti–7.5Mo that were not alkali-treated, and the surface of Ti–7.5Mo without alkali treatment showed no obvious changes, even after 28 days of immersion in the SBF. For the surface of c.p. Ti under the same conditions, the porous structures formed by acid etching were slightly more denser after immersion in SBF for 28 days when compared with those before the immersion.

Figures 4 and 5 show the SEM micrographs of the surface morphology of acid-etched and NaOH-treated c.p. Ti and Ti–7.5Mo substrates after soaking for different intervals in SBF. As shown in the micrographs, apatite began to deposit on acid-etched and NaOH-treated Ti–7.5Mo within 1 day after immersion in SBF, which was much faster than in the case of c.p. Ti, as there were no precipitations on the surfaces of the c.p. Ti substrates after the same period of time. Moreover, the apatite began to deposit within 3 days after immersion of the only NaOH-treated samples [59]. After 7 days in the SBF, a few tiny Ca–P particles with a diameter of less than 1 μm were sparsely deposited on the surface of the c.p. Ti, whereas, after the same period of time, a greater number of spheroid particles about the same size were observed on the surfaces of the Ti–7.5Mo. After immersion for 14 days, the surfaces of all the samples were mostly covered by a newly foamed layer of Ca–P composed of island-like spherulites. Significantly, there were more aggregate spherulites deposited on the surfaces of HCl-etched metals than on those treated with H_3PO_4. However, all the pretreated surfaces induced some island-like particles to grow on them, and the area covered by such particles gradually increased with an increase in immersion time. The final coatings after 28 days of immersion in the SBF (Figs. 4g, h and 5g, h) indicated that a dense

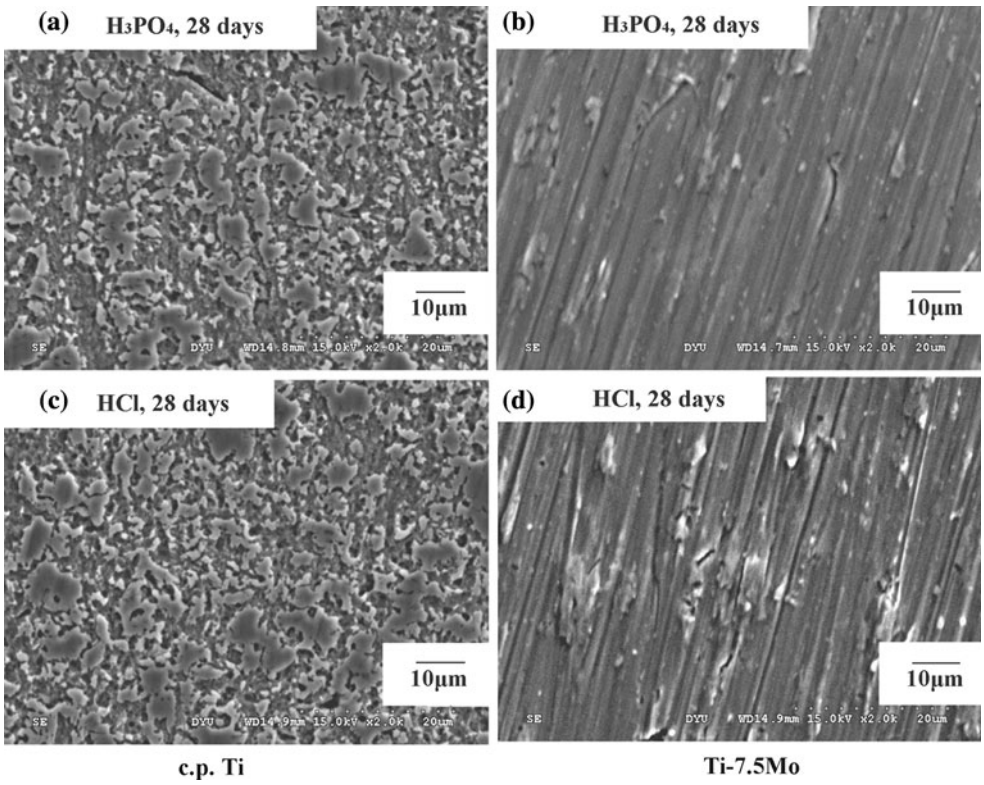

Fig. 3 SEM micrographs of surface morphology of acid-etched c.p. Ti (*left*) and Ti–7.5Mo (*right*) after soaking in SBF for 28 days

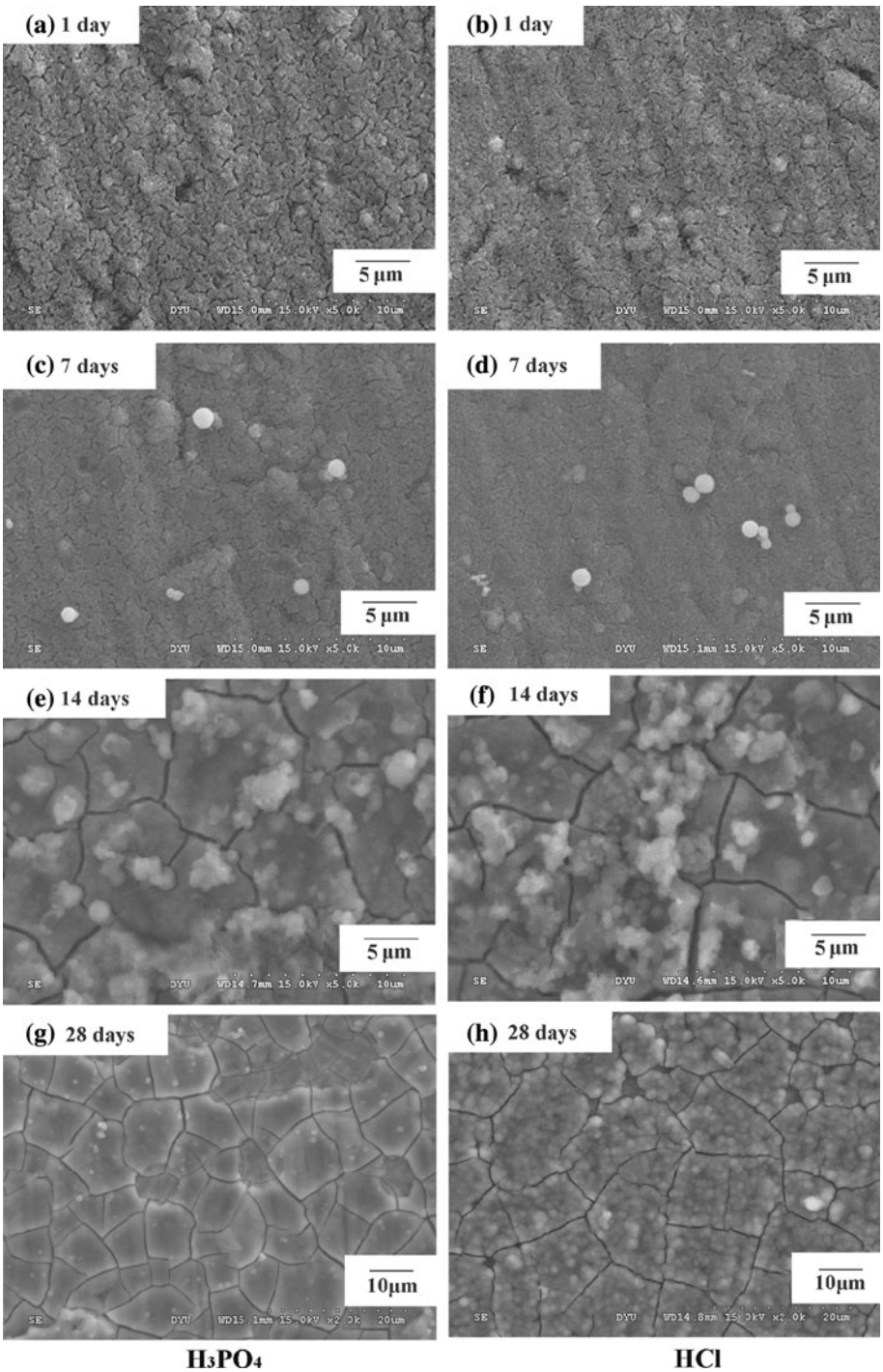

Fig. 4 SEM micrographs of surface morphology of H_3PO_4-etched (*left*) or HCl-etched (*right*) and subsequently NaOH-treated c.p. Ti after various soaking periods in SBF

and newly formed uniform layer was produced on the surfaces of all the acid-etched and alkali-treated c.p. Ti and Ti–7.5Mo. It is noteworthy that the formation of Ca–P layers with a similar morphology has been reported for Ti and several of its alloys [50, 60, 61]. Finally, the cracks in the Ca–P layer on the c.p. Ti and Ti–7.5Mo appear to have formed as a result of contraction of the porous-hydrated layer when the specimens were dried after being soaked in SBF.

According to the literatures [62, 63], Ti and its alloys form sodium titanate hydrogel layers on their surfaces after NaOH treatment. Immediately after being soaked in SBF, Na^+ ions from the sodium titanate layer are exchanged by H_3O^+ ions from the surrounding fluid, thereby resulting in the formation of a Ti–OH layer. The released Na^+ ions increase the degree of supersaturation of the soaking solution, and Ti–OH groups induce apatite nucleation on the Ti surface. Therefore, the low

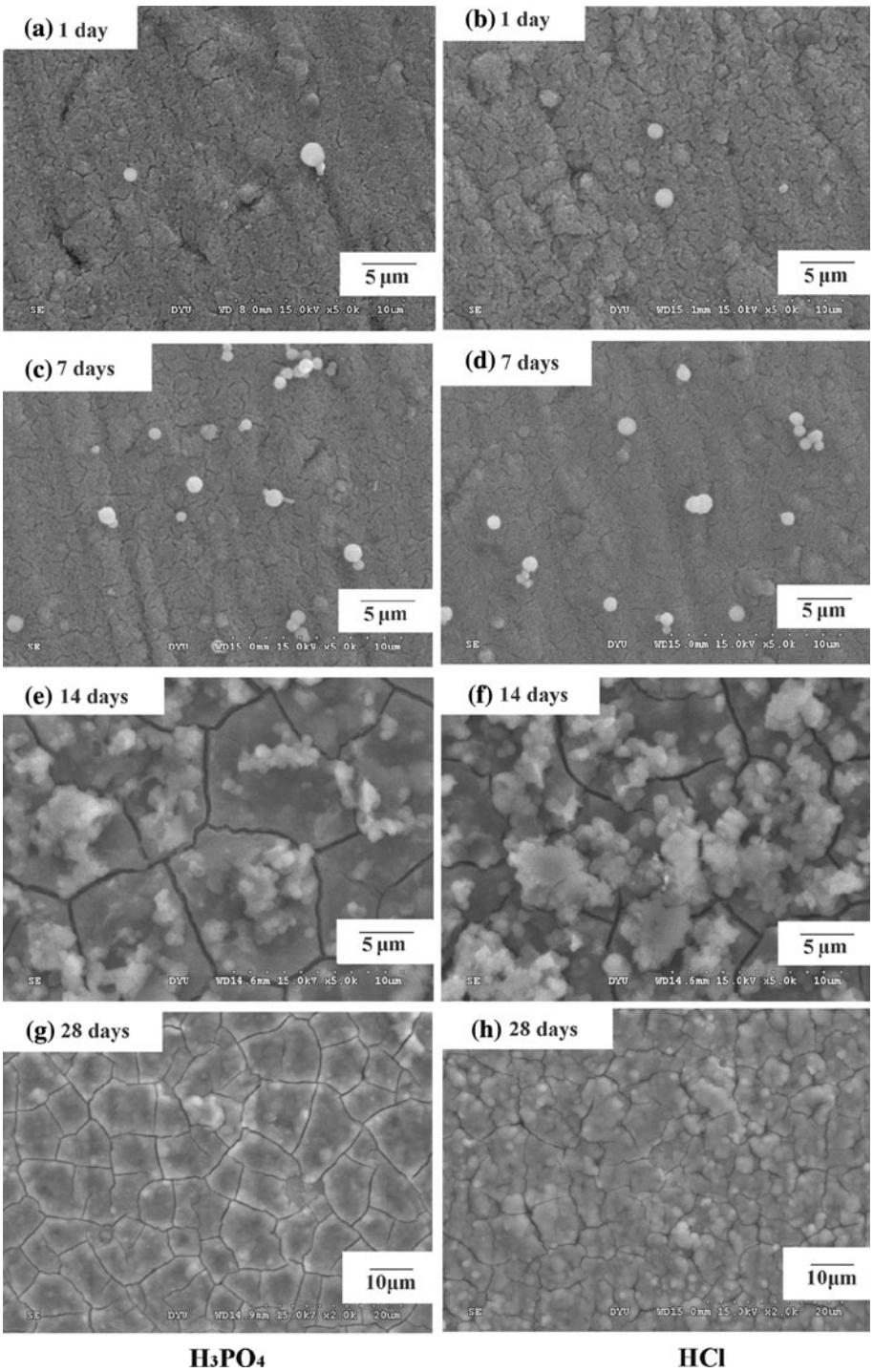

Fig. 5 SEM micrographs of surface morphology of H_3PO_4-etched (*left*) or HCl-etched (*right*) and subsequently NaOH-treated Ti–7.5Mo after various soaking periods in SBF

apatite-forming ability of the acid-etched and alkali-treated c.p. Ti may be attributed to the smaller amount of Na^+ ions in the surface gel layer on the c.p. Ti, which is in agreement with the results of the XRD (figure not shown).

The results of the EDS (Fig. 6a) show that Ca and P can be detected when specimens of acid-etched and NaOH-treated c.p. Ti and Ti–7.5Mo are soaked in SBF for 28 days. HCl-etched and NaOH-treated c.p. Ti and Ti–7.5Mo specimens both exhibited very intensive peaks of Ca and P. Moreover, the intensity of the substrate Ti dramatically decreased due to interference from the Ca–P deposits after being soaked in SBF. In a recent study by Müller et al. [64], sintered Ti–13Nb–13Zr samples were etched in HCl, H_3PO_4, or in a mixture of HF + HNO_3, respectively, and subsequently treated in NaOH. Notably, the results also

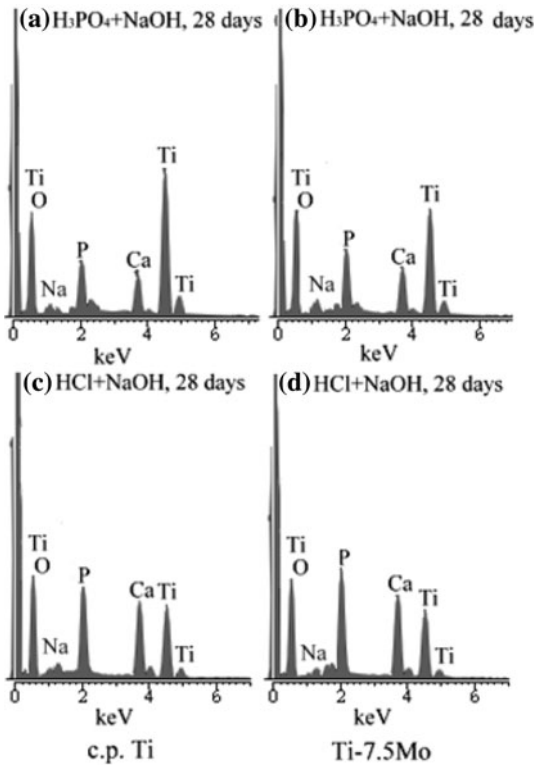

Fig. 6 EDS analysis of acid-etched and NaOH-treated c.p. Ti (*left*) and Ti–7.5Mo (*right*) after soaking in SBF for 28 days

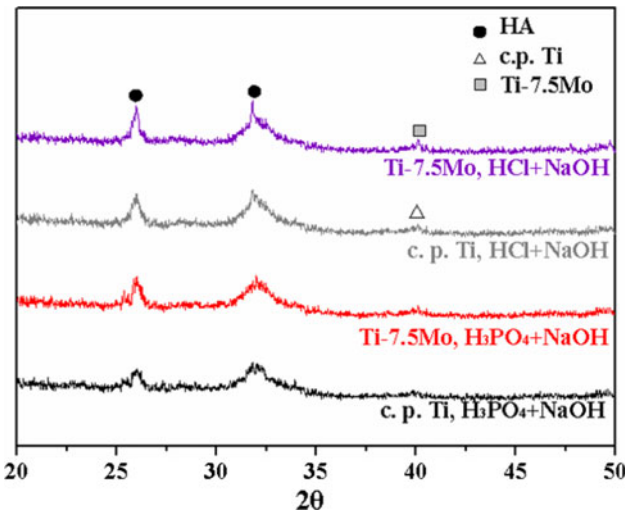

Fig. 7 XRD patterns of acid-etched and NaOH-treated c.p. Ti and Ti–7.5Mo after soaking in SBF for 28 days

showed that the HA formation rate was the highest for HCl-pretreated samples.

Figure 7 shows the thin film XRD patterns of acid-etched and NaOH-treated c.p. Ti and Ti–7.5Mo surfaces after soaking in SBF for 28 days. Peaks of HA appear on all the patterns, but the intensities of the peaks are greater for the Ti–7.5Mo specimens. Additionally, after being soaked in SBF for 28 days, the intensities of the c.p. Ti and Ti–7.5Mo substrates dramatically decreased due to interference from Ca–P deposits.

In comparable studies [65, 66] in which the method of etching with a mixture of HCl and H_2SO_4 followed by immersion in boiling dilute NaOH solution was evaluated, it was found that the microporous titanium oxide surface layer formed by the treatment allowed fast precipitation of apatite. Moreover, Jonášová et al. [67] found that acid etching of Ti in HCl leads to the formation of a uniform micro-roughened surface that provides improved conditions for in situ Ca–P formation. However, in this study, the surface of Ti–7.5Mo did not show a porous structure after acid etching of H_3PO_4 or HCl. However, it is noteworthy that the apatite deposition was much quicker for Ti–7.5Mo than for c.p. Ti. In our previous study [59], the apatite did not start to deposit on the NaOH-treated samples until the third day after their immersion. However, in this present experiment when a combination of both acid etching and alkaline treatment was used for Ti–7.5Mo, the apatite began to deposit within 1 day after immersion in the SBF. Consequently, c.p. Ti and Ti–7.5Mo subjected to both acid etching and alkaline treatment show a greater level of high apatite-forming ability than that of c.p. Ti and Ti–7.5Mo subjected to only NaOH treatments. This is important because the speed and quality of newly formed bonelike apatite are critical in determining the early implant–bone integration. Fast fixation can reduce hospitalization time and costs and improve quality of life for patients. From this point of view, selecting a suitable surface treatment to obtain the fast apatite deposition from SBF is meaningful and could be a guide for future consideration during bone replacement surgery.

Conclusions

(1) The surfaces of acid-etched c.p. Ti showed a porous structure; however, those of acid-etched Ti–7.5Mo showed flat surfaces with some grinding marks. After subsequent alkali treatment in NaOH, the surfaces of both the c.p. Ti and Ti–7.5Mo substrates exhibited microporous network structures.

(2) After acid etching in H_3PO_4 or HCl, the water-contact angles of the surfaces slightly decreased. The water-contact angles of the surfaces of the c.p. Ti and Ti–7.5Mo became even smaller after acid etching and subsequent NaOH treatment. Additionally, the Ti–7.5Mo surfaces have the lowest contact angles after HCl etching in combination with the NaOH treatment.

(3) Apatite began to deposit on acid-etched and NaOH-treated Ti–7.5Mo within 1 day after immersion of in

SBF—much faster than in the cases involving c.p. Ti. After immersion for 7 days, more spheroid particles with diameters less than 1 μm were observed on the surfaces of the acid-etched and NaOH-treated Ti–7.5Mo. After immersion for 14 days, there were more aggregate spherulites deposited on the surfaces of HCl-etched metals than on those treated with H_3PO_4. After 28 days of immersion in the SBF a dense and uniform layer was produced on the surface of all the acid-etched and alkali-treated c.p. Ti and Ti–7.5Mo samples.

(4) A combination of acid etching and subsequent NaOH treatment was successfully used to initiate in vitro apatite formation on the surface of Ti–7.5Mo alloys. The rate of HA formation was the highest for those samples etched in HCl.

Acknowledgement This study was partially supported by a grant, NSC 97-2815-C-212-014-E, provided by National Science Council of Taiwan.

References

1. Yan WQ, Davies JE (1998) Bioceramics 11:659
2. Nishiguchi S, Nakamura T, Kobayashi M, Kim HM, Miyaji F, Kokubo T (1999) Biomaterials 20:491
3. Morris HF, Ochi S, Spray JR, Olson JW (2000) Ann Periodontol 5:56
4. Geurs NC, Jeffcoat RL, McGlumphy EA, Reddy MS, Jeffcoat MK (2002) Int J Oral Maxillofac Implants 17:811
5. Barrère F, Van der Valk CM, Meijer G, Dalmeijer RAJ, De Groot K, Layrolle P (2003) J Biomed Mater Res 67B:655
6. Ong JL, Lucas LC, Lacefield WR, Rigney ED (1992) Biomaterials 13:249
7. Ducheyne P, Radin S, Heughebaert M, Heughebaert JC (1990) Biomaterials 11:244
8. Albayrak O, El-Atwani O, Altintas S (2008) Surf Coat Technol 202:2482
9. Boyd AR, Duffy H, McCann R, Meenan BJ (2008) Mater Sci Eng C 28:228
10. Im KH, Lee SB, Kim KM, Lee YK (2007) Surf Coat Technol 202:1135
11. De Groot K, Geesink RGT, Klein CPAT, Serekian P (1987) J Biomed Mater Res 21:1375
12. Klein CAPT, Patka P, Van der Lubbe HBM, Wolke JGC, De Groot K (1991) J Biomed Mater Res 25:53
13. Pilliar RM (2005) Orthop Clin North Am 36:113
14. Radin SR, Ducheyne P (1992) J Mater Sci Mater Med 3:33
15. Weng J, Liu X, Zhang X, De Groot K (1996) J Biomed Mater Res 30A:5
16. Ikawa N, Oumi Y, Kimura T, Ikeda T, Sano T (2008) J Mater Sci 43:4198. doi:10.1007/s10853-008-2602-5
17. Neira IS, Guitián F, Taniguchi T, Watanabe T, Yoshimura M (2008) J Mater Sci 43:2171. doi:10.1007/s10853-007-2032-9
18. Yunos DM, Bretcanu O, Boccaccini AR (2008) J Mater Sci 43:4433. doi:10.1007/s10853-008-2552-y
19. Costa HS, Mansur AAP, Barbosa-Stancioli EF, Pereira MM, Mansur HS (2008) J Mater Sci 43:510. doi:10.1007/s10853-007-1849-6
20. MacKenzie KJD, Rahner N, Smith ME, Wong A (2010) J Mater Sci 45:999. doi:10.1007/s10853-009-4031-5
21. Li P, Ohtsuki C, Kokubo T, Nakanishi K, Soga N, De Groot K (1994) J Biomed Mater Res 28:7
22. Li P, Kangasniemi I, De Groot K, Kokubo T (1994) J Am Ceram Soc 5:1307
23. Ohtsuki C, Iida H, Hayakawa S, Osaka A (1997) J Biomed Mater Res 35:39
24. Wang XX, Hayakawa S, Tsuru K, Osaka A (2000) J Biomed Mater Res 52:171
25. Kaneko S, Tsuru K, Hayakawa S, Takemoto S, Ohtsuki C, Ozaki T, Inoue H, Osaka A (2001) Biomaterials 22:875
26. Wu JM, Hayakawa S, Tsuru K, Osaka A (2004) J Am Ceram Soc 87:1635
27. Kim HM, Miyaji F, Kokubo T, Nishiguchi S, Nakamura T (1999) J Biomed Mater Res 45:100
28. Nishiguchi S, Kato H, Fujita H, Oka M, Kim HM, Kokubo T, Nakamura T (2001) Biomaterials 22:2525
29. Uchida M, Kim HM, Kokubo T, Fujibayashi S, Nakamura T (2002) J Biomed Mater Res 63B:522
30. Habibovic P, Li J, Van der Valk CM, Meijer G, Layrolle P, Van Blitterswijk CA, De Groot K (2005) Biomaterials 26:23
31. Trentani L, Pelillo F, Pavesi FC, Ceciliani L, Cetta G, Forlino A (2002) Biomaterials 23:2863
32. Lin DJ, Chern Lin JH, Ju CP (2002) Biomaterials 23:1723
33. Ho WF, Chiang TY, Wu SC, Hsu HC (2009) J Alloys Compd 468:533
34. Okazaki Y, Nishimura E (2000) Mater Trans 41:1247
35. Okazaki Y, Rao S, Ito Y, Tateishi T (1998) Biomaterials 19:1197
36. Oliveira NTC, Ferreira EA, Duarte LT, Biaggio SR, Rocha-Filho RC, Bocchi N (2006) Electrochim Acta 51:2068
37. Hao YL, Li SJ, Sun SY, Zheng CY, Yang R (2007) Acta Biomater 3:277
38. Pipino F (2000) J Orthop Traumatol 1:3
39. Sumner DR, Galante JO (1992) Clin Orthop Relat Res 274:202
40. Cheal E, Spector M, Hayes W (1992) J Orthop Res 10:405
41. Ho WF (2008) J Alloys Compd 464:580
42. Ho WF, Ju CP, Chern Lin JH (1999) Biomaterials 20:2115
43. Lin DJ, Chuang CC, Chern Lin JH, Lee JW, Ju CP, Yin HS (2007) Biomaterials 28:2582
44. Faure J, Balamurugan A, Benhayoune H, Torres P, Balossier G, Ferreira JMF (2009) Mater Sci Eng C 29:1252
45. Kokubo T (1999) Biomaterials 12:155
46. Hench LL (1991) J Am Ceram Soc 74:1487
47. Li P, Ohtsuki C, Kokubo T, Nakanishi K, Soga N, Nakamura N, Yamamuro T (1993) J Mater Sci Mater Med 4:127
48. Zardiackas LD, Mitchell DW, Disegi JA (1996) In: Brown SA, Lemons JE (eds) Medical applications of titanium and its alloys. ASTM, West Conshohocken
49. Sakaguchi S, Nakahara K, Hayashi Y (1999) Met Mater Int 5:193
50. Kim HM, Miyaji F, Kokubo T, Nakamura T (1996) J Biomed Mater Res 32:409
51. Vogler EA, Graper JC, Harper GR, Lander LM, Brittain WJ (1995) J Biomed Mater Res 29:1005
52. Lee JH, Lee HB (1998) J Biomed Mater Res 41:304
53. Choee JH, Lee SJ, Lee YM, Rhee JM, Lee HB, Khang G (2004) J Appl Polym Sci 92:599
54. Faucheux N, Schweiss R, Lutzow K, Werner C, Groth T (2004) Biomaterials 25:2721
55. Buser D, Broggini N, Wieland M, Schenk RK, Denzer AJ, Cochran DL, Hoffmann B, Lussi A, Steinemann SG (2004) J Dent Res 83:529
56. Zhao G, Schwartz Z, Wieland M, Rupp F, Geis-Gerstorfer J, Cochran DL, Boyan BD (2005) J Biomed Mater Res 74A:49
57. Bagno A, Di Bello C (2004) J Mater Sci Mater Med 15:935

58. Giavaresi G, Fini M, Cigada A, Chiesa R, Rondelli G, Rimondini L, Torricelli P, Aldini NN, Giardino R (2003) Biomaterials 24:1583
59. Ho WF, Lai CH, Hsu HC, Wu SC (2009) Surf Coat Technol 203:3142
60. Kim HM, Takadama H, Miyaji F, Kokubo T, Nishiguchi S, Nakamura T (2000) J Mater Sci Mater Med 11:555
61. Rosenberg R, Starosvetsky D, Gotman I (2003) J Mater Sci Lett 22:29
62. Takadama H, Kim HM, Kokubo T, Nakamura T (2001) J Biomed Mater Res 57:441
63. Kokubo T (1996) Thermochim Acta 280–281:479
64. Müller FA, Bottino MC, Müller L, Henriques VAR, Lohbauer U, Bressiani AHA, Bressiani JC (2008) Dent Mater 24:50
65. Brown M, Gregson PJ, West RH (1996) J Mater Sci Mater Med 7:323
66. Martin JY, Schwartz Z, Hummert TW, Schraub DM, Simpson J, Lankford J, Dean DD, Cochran DL, Boyan BD (1995) J Biomed Mater Res 29:389
67. Jonášová L, Müller FA, Helebrant A, Strnad J, Greil P (2004) Biomaterials 25:1187